

Electronic structure of $\text{SrRu}_{1-x}\text{Mn}_x\text{O}_3$ studied by photoemission and x-ray absorption spectroscopy

K. Horiba,^{1,*} H. Kawanaka,² Y. Aiura,² T. Saitoh,³ C. Satoh,⁴ Y. Kikuchi,⁴ M. Yokoyama,⁴ Y. Nishihara,⁴ R. Eguchi,¹ Y. Senba,⁵ H. Ohashi,⁵ Y. Kitajima,⁶ and S. Shin^{1,7}

¹RIKEN SPring-8 Center, Sayo-cho, Sayo-gun, Hyogo 679-5148, Japan

²National Institute of Advanced Industrial Science and Technology, Tsukuba, Ibaraki 305-8568, Japan

³Department of Applied Physics, Tokyo University of Science, Shinjuku-ku, Tokyo 162-8601, Japan

⁴Faculty of Science, Ibaraki University, Mito, Ibaraki 310-8512, Japan

⁵JASRI/SPring-8, Sayo-cho, Hyogo 679-5198, Japan

⁶Photon Factory, High Energy Accelerator Research Organization, Tsukuba, Ibaraki 305-0801, Japan

⁷Institute for Solid State Physics, The University of Tokyo, Kashiwa, Chiba 277-8581, Japan

(Received 8 February 2010; revised manuscript received 11 June 2010; published 28 June 2010)

In order to investigate the change in the electronic structure with Mn doping of $\text{SrRu}_{1-x}\text{Mn}_x\text{O}_3$ (SRMO), we have performed soft x-ray synchrotron photoemission spectroscopy (PES) and x-ray absorption spectroscopy (XAS). In the soft x-ray PES spectra, the sharp peak structure near the Fermi level (E_F), which was clearly observed in SrRuO_3 , was suppressed accompanied with Mn doping in SRMO. In the Mn $2p$ XAS and Mn $2p$ - $3d$ resonant PES spectra, we have confirmed the existence of Mn^{3+} ions with the electron doping to Mn $3d$ e_g states and Mn $3d$ partial density of state never have finite intensity at E_F in SRMO. These results suggest that the metal-insulator transition of SRMO with Mn doping is originated from the charge transfer from the itinerant Ru $4d$ t_{2g} bands to the localized Mn $3d$ e_g orbitals.

DOI: [10.1103/PhysRevB.81.245127](https://doi.org/10.1103/PhysRevB.81.245127)

PACS number(s): 71.30.+h, 79.60.-i

Perovskite-type transition-metal oxides (TMOs) have attracted much attention because of their unique physical phenomena such as colossal magnetoresistance, percolation, phase separation, etc., resulting from the strongly correlated d -band electrons and hybridization between the transition-metal d bands and O $2p$ bands.^{1,2} The ruthenates, as a class of TMOs exhibit a wide variety of physical properties derived from the itinerant-localized duality of Ru $4d$ electrons. SrRuO_3 (SRO) is known well to be an itinerant ferromagnetic metal (FM) with the Curie temperature of around 160 K. The substitution of $3d$ -metal ions for the Ru ions causes the localization of d electrons, electronic disorders, and charge transfer between the Ru ions and $3d$ -metal ions. Correlations among these phenomena result in the various physical properties such as metal-insulator and magnetic transitions in $3d$ -doped $\text{SrRu}_{1-x}\text{M}_x\text{O}_3$ ($M=\text{Ti, Cr, Mn, Fe, etc.}$) system.³⁻¹⁴

The one of the most striking compounds in the system is Mn-doped $\text{SrRu}_{1-x}\text{Mn}_x\text{O}_3$ (SRMO).⁷⁻¹⁴ The other end of SRMO compounds, SrMnO_3 (SMO) is an antiferromagnetic (AF) insulator, which is originated from localized Mn $3d$ t_{2g} electrons since SMO has only Mn^{4+} ions which have no Mn $3d$ e_g electrons. Many investigations for unusual physical properties in the intermediate compositions of SRMO system have been reported.⁷⁻¹⁴ Cao *et al.*⁷ reported on single-crystalline samples of SRMO that the Mn doping suppresses the itinerant ferromagnetic phase, and then induces a new insulating phase above the critical point $x_c=0.39$. For $x>x_c$, the temperature variations in the magnetic susceptibility suggest the appearance of AF order in the insulating phase. On the other hand, Sahu *et al.*⁸ reported on the polycrystalline samples that the ferromagnetic state is still stable up to $x=0.5$. They also mentioned the charge transfer between Ru and Mn ions from the results of x-ray absorption spectroscopy (XAS). Recently, Yokoyama *et al.*⁹ found using powder neutron-diffraction measurements that the itinerant ferromagnetic order in SRO changes into the AF order with nearly localized d electrons in the intermediate Mn-concentration range between $x=0.4$ and 0.6 . Kolesnik *et al.*¹² states the existence of spin-glass phase between the ferromagnetic-to-antiferromagnetic transition. Thus, basically the physical properties of SRMO have been understood as itinerant FM in the low Mn-doping region, and as AF insulators in the high Mn-doping region. However, the detailed behaviors near the transition compositions are still controversial and the mechanism of the transitions is not clear.

In order to clarify the origin of complicated physical properties in Mn-substituted SRO, it is important to understand the electronic structure of SRMO. In particular, observation of change in the element-selective electronic structure accompanied with Mn substitution for Ru in SRMO provides us with direct information on hybridization and charge transfer between Ru and Mn ions. XAS and resonant photoemission spectroscopy (PES) are very powerful techniques to observe such element-selective electronic structure of solids. In this work, we perform the soft x-ray synchrotron PES and XAS to elucidate the origin of the metal-insulator transition of SRMO with Mn doping.

Polycrystalline SRMO samples were prepared by conventional solid-state reaction methods⁹ with the starting materials of SrCO_3 , RuO_2 , and MnO . The samples with stoichiometric compositions were first calcined at 750°C for 4 h and shaped into pellets. They were then sintered at 1300°C for 24 h in the ambient atmosphere. In order to avoid contamination of impurity phases, we iterated the sintering process tenfold. All the SRMO samples were confirmed to consist of a single phase within the experimental accuracy by

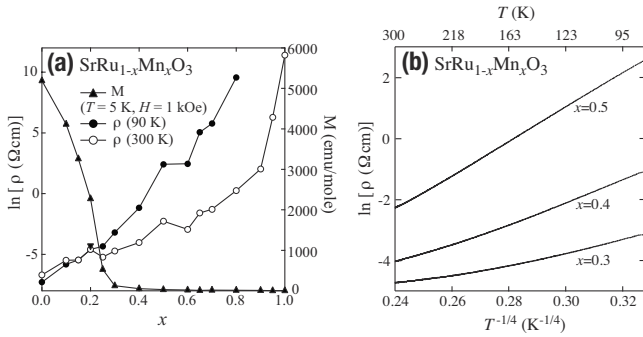


FIG. 1. (a) Mn-concentration dependence of resistivity (at 300 and 90 K) and magnetization at 5 K of SrRu_{1-x}Mn_xO₃. (b) Resistivity in a logarithmic scale as a function of T^{-1/4} of SrRu_{1-x}Mn_xO₃ (x=0.3, 0.4, and 0.5). In case of a three-dimensional variable-range hopping conduction, the temperature dependence of the resistivity can be described with the formula $\rho(T)=\rho_0 \exp(T_0/T)^{1/4}$.

x-ray powder-diffraction measurements. Electrical resistivity and magnetization were measured by the four-probe method and a superconducting quantum interference device magnetometer, respectively.

PES and Mn L-edge XAS study were carried out using the high-resolution PES apparatus at beamline BL17SU of SPring-8 (Ref. 15) and Ru L-edge XAS experiments were performed at BL-11B of Photon Factory, KEK. All measurements were performed at room temperature. The clean surface of the samples was obtained by fractured *in situ*. XAS spectra were obtained with total electron yield mode by measuring the sample drain current. The total-energy resolution of PES and Mn L-edge XAS measurements was set to 200 meV, and that of Ru L-edge XAS measurements was 1.5 eV.

The Mn-concentration dependence of magnetic and transport properties are shown in Fig. 1. The magnetization has decreased rapidly by the Mn substitution and ferromagnetism seems to have disappeared in the vicinity of x~0.3. The temperature dependence of the resistivity shows that the variable-range hopping (VRH) conduction becomes predominant over the metallic conduction with increasing Mn substitution.¹¹ The disappearance of the itinerant-electron ferromagnetism and the appearance of the AF order were observed in the neutron-diffraction measurements on x ≥ 0.4.⁹ From these transport and magnetic results, the transition from the band metal conduction to the VRH conduction was found to be corresponding to the transition from the itinerant-electron ferromagnetism to the AF order.

Figure 2 shows Mn L-edge and Ru L-edge XAS spectra of SRMO. With increasing Mn doping, the main peaks for both Mn L-edge and Ru L-edge XAS spectra shift to a higher energy and new shoulder structures appear at the lower-energy side. The spectral changes are very similar to those in the previous report.⁸ Compared with the spectral shape of the Mn L-edge XAS spectra for La_{1-x}Sr_xMnO₃ (LSMO) with the intermediate composition^{16,17} and MnO₂ (Ref. 17) as a reference of Mn⁴⁺, it is found that Mn³⁺ and Mn⁴⁺ ions are dominant in the Mn-poor region and the Mn-rich region of SRMO, respectively, in spite of the homovalent doping. In the Mn-poor region, since only a small part of the majority Ru⁴⁺ ions give electrons to the minority Mn⁴⁺ ions, it is

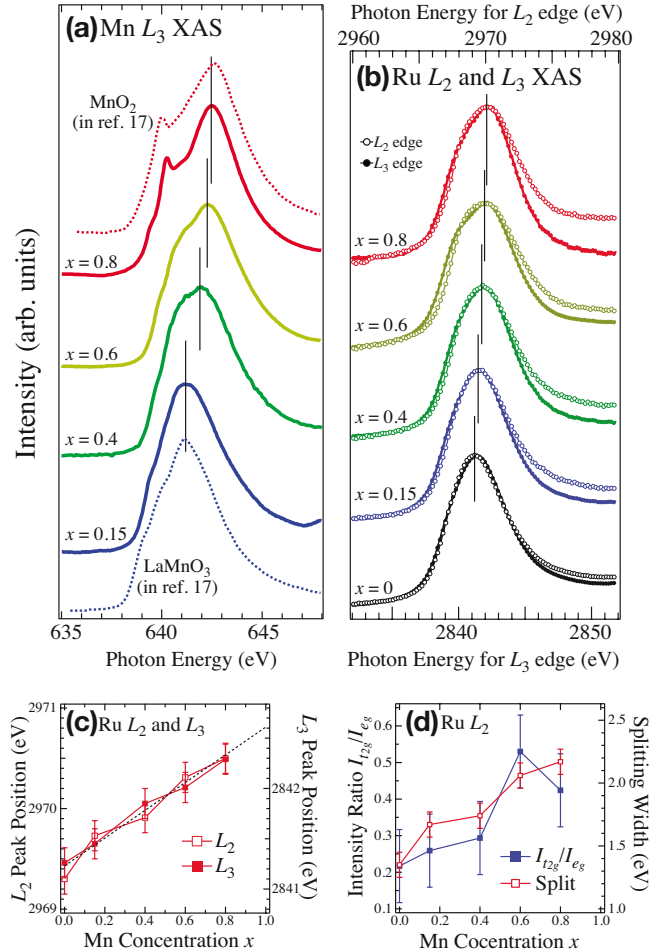


FIG. 2. (Color online) (a) Mn L₃ XAS spectra of SrRu_{1-x}Mn_xO₃. XAS spectra LaMnO₃ and MnO₂ taken from Ref. 17 are also shown as references of Mn³⁺ and Mn⁴⁺, respectively. In order to consider only the spectral shapes and the relative energy shift, the both reference spectra are shown with shift of 2.8 eV to lower photon energy. (b) Ru L₂ and Ru L₃ XAS spectra of SrRu_{1-x}Mn_xO₃. (c) Mn-concentration dependence of the peak position of Ru L₂ and Ru L₃ XAS spectra of SrRu_{1-x}Mn_xO₃. (d) Mn-concentration dependence of the splitting width and the intensity ratio between t_{2g} and e_g components in Ru L₂ XAS spectra of SrRu_{1-x}Mn_xO₃.

observed in the XAS spectra that the Mn³⁺ ions are dominant and Ru⁴⁺ ions remains. On the other hand, in the Mn-rich region, the minority Ru⁴⁺ ions give electrons to only a small part of the majority Mn⁴⁺ ions and dominant Mn⁴⁺ and Ru⁵⁺ ions are observed in the XAS spectra. In short, these XAS results indicate that charge redistribution from Ru⁴⁺-Mn⁴⁺ to Ru⁵⁺-Mn³⁺ occurs in SRMO.⁸

It is difficult to estimate Mn valency quantitatively for the intermediate composition of SRMO because of the complicated multiplet structures in Mn³⁺ L- and Mn⁴⁺ L-edge XAS spectra. On the other hand, concerning Ru L-edge XAS spectra, the quantitative estimation of Ru valency from the detailed analysis of Ru L-edge XAS spectra on La_{2-x}Sr_xCu_{1-y}Ru_yO_{4-δ} have been reported.¹⁸ According to this report, the main peak position and the intensity ratio between the doubled-peak structures derived from Ru 4d t_{2g}

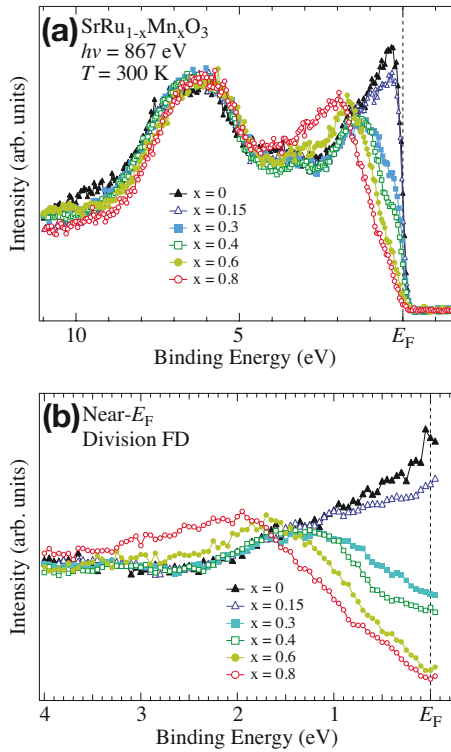


FIG. 3. (Color online) (a) Valence-band PES spectra of SrRu_{1-x}Mn_xO₃ taken at the photon energy of 867 eV. (b) Near- E_F spectra divided by Fermi-Dirac functions convolved with the experimental resolution and thermal broadening estimated by the gold spectra at the same experiments.

and e_g orbitals in Ru L -edge XAS spectra are proportional well to the Ru valency and therefore these are useful as indicators for the Ru valency. Figures 2(c) and 2(d) show analytical results on Ru L -edge XAS spectra of SRMO. If the Ru and Mn ions are ordered alternately in SRMO, that charge redistribution from Ru⁴⁺-Mn⁴⁺ to Ru⁵⁺-Mn³⁺ is completed at $x=0.5$ and the Ru valency keep Ru⁵⁺ in the Mn-rich region. Therefore, the systematic change in Ru valency in the whole range of Mn concentrations suggests that the Ru and Mn ions are placed at random in SRMO.

In order to clarify the change in the density of states (DOS) accompanied with the charge redistribution in SRMO, we have performed PES measurements. Figure 3 shows valence-band PES spectra of SRMO taken at the photon energy of 867 eV. The photoionization cross section of O $2p$, Mn $3d$, and Ru $4d$ orbitals in 867 eV are about 0.1, 1, and 10, respectively.¹⁹ Therefore the valence-band spectra taken at 867 eV are mostly contributed from the Ru $4d$ orbital at least for the Ru-rich region of SRMO samples. Ru $4d$ -O $2p$ hybridized bands at around 6 eV does not show any significant change for all compositions of SRMO, suggesting that SRMO samples keep the perovskite structure without serious distortions by Mn substitution. Ru $4d$ -derived bands near the Fermi level (E_F) split into two states, just below E_F and at around 1.5 eV. In the SRO spectrum, strong spectral intensity of the states just below E_F is observed, reflecting the high conductivity of SRO. In contrast, the intensity of the states just below E_F is suppressed in the spectra of SRMO accom-

panied with the substitution of Mn for Ru. This intensity change at E_F can be more emphasized by dividing the spectra by Fermi-Dirac function as shown in Fig. 3(b). The reduction in the spectral intensity at E_F is most drastically in between SRMO with $x=0.15$ and 0.3, probably corresponding to the metal-insulator transition around $x=0.3$ observed by the transport measurements.⁹ However, even SRMO with $x=0.4$, which shows the insulating properties in resistivity, finite DOS remains at E_F . Since the finite DOS in SRMO with $x=0.4$ is also observed in highly bulk-sensitive hard x-ray PES measurements,²⁰ this is not a surface problem. This suggests the possibility of electronic phase separation between isolated metallic islands and spread-insulating regions.²¹

In contrast to the strong intensity suppression at E_F with Mn doping, the spectral weight of the states around 1.5 eV does not increase in the spectra of SRMO system with between $x=0$ and $x=0.4$. In bandwidth control system perovskite ruthenium oxides Ca_{1-x}Sr_xRuO₃ (CSRO), the spectral weight transfer from coherent states to incoherent states have been observed with increasing the correlation strength.²² The difference between SRMO and CSRO system suggests that the origin of the reduced DOS at E_F in SRMO with Mn doping is not the increase in correlation strength with narrowing the Ru $4d$ bands but reduction in itinerant Ru $4d$ carriers with trapping the Ru $4d$ electrons in other sites.

The contribution of Mn $3d$ counterpart can be extracted from the valence band by using Mn $2p$ - $3d$ resonant PES technique. Resonant PES spectra of SRMO samples are shown in Fig. 4. The photon energies for the on-resonance condition are determined from the peak position of Mn L_3 x-ray absorption edge at each samples as shown in Fig. 2(a). The off-resonance condition is fixed at 635 eV. Differences between the on-resonance and off-resonance spectra as summarized in Fig. 4(e) correspond to Mn $3d$ partial DOS of SRMO. In comparison with the resonant PES spectra of LSMO,²³ the structures around 2 eV and near E_F are assigned to Mn $3d$ t_{2g} and Mn $3d$ e_g states, respectively. The intensity of Mn $3d$ e_g states is proportional to the amount of the Mn³⁺ valence state.²³ The increase in Mn $3d$ e_g states with increasing Ru ions, hence, strongly indicates the charge transfer from Ru $4d$ to Mn $3d$ in SRMO, and is good agreement with the XAS results in Fig. 2.

In addition, from the detailed analysis of resonant PES spectra in the near- E_F region, we find that Mn $3d$ partial DOS never have finite intensity at E_F in all composition of SRMO, in contrast to the Ru $4d$ -derived states [see Fig. 4(e)]. These results suggest that the transferred Mn $3d$ e_g electrons from the Ru $4d$ t_{2g} bands are localized and do not contribute to conductivity of SRMO.

The summarized diagrams of the electronic structure of SRMO obtained from all results of PES, XAS, and resonant PES are shown in Fig. 5. In the end compounds SRO and SMO, transition-metal ions exist in the form of Ru⁴⁺ ($4d$ t_{2g}^4) and Mn⁴⁺ ($3d$ t_{2g}^3), respectively. From the results of PES spectra, Ru $4d$ t_{2g} bands of SRO split into coherent (itinerant) and incoherent (localized) components while all Mn $3d$ t_{2g} electrons in SMO is expected to be localized. When these compounds are mixed as SRMO, charge transfer occurs from the Ru $4d$ itinerant bands to Mn $3d$ orbitals. The

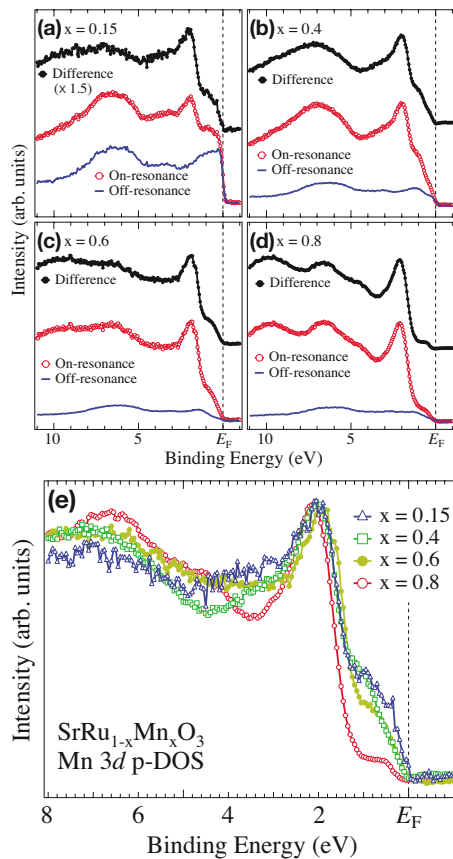


FIG. 4. (Color online) Mn $2p$ - $3d$ resonant PES spectra of $\text{SrRu}_{1-x}\text{Mn}_x\text{O}_3$ with (a) $x=0.15$, (b) $x=0.4$, (c) $x=0.6$, and (d) $x=0.8$. On-resonance spectra were measured at the photon energy of Mn L_3 absorption edge indicated by straight lines in Fig. 2(a). Off-resonance spectra were measured at 635 eV. (e) Comparison of Mn $3d$ partial DOS with different composition taken by subtraction of the off-resonance spectra from the on-resonance spectra in (a)–(d). All spectra are normalized by the intensity of distinctive Mn $3d$ t_{2g} -derived peaks around 2 eV.

transferred Mn $3d$ electrons get into Mn $3d$ e_g orbitals and are localized. The appearance of inhomogeneous localized states with Mn doping is consistent with the VRH conduction near the metal-insulator transition of SRMO. Altogether, it is concluded that the suggested origin of metal-insulator transition of SRMO with Mn doping is the charge transfer from the itinerant Ru $4d$ t_{2g} bands to the localized Mn $3d$ e_g orbitals, and consequently the interrupt of the itinerancy of Ru $4d$ electrons by localized Mn $3d$ states.

In conclusion, we have carried out the PES and XAS

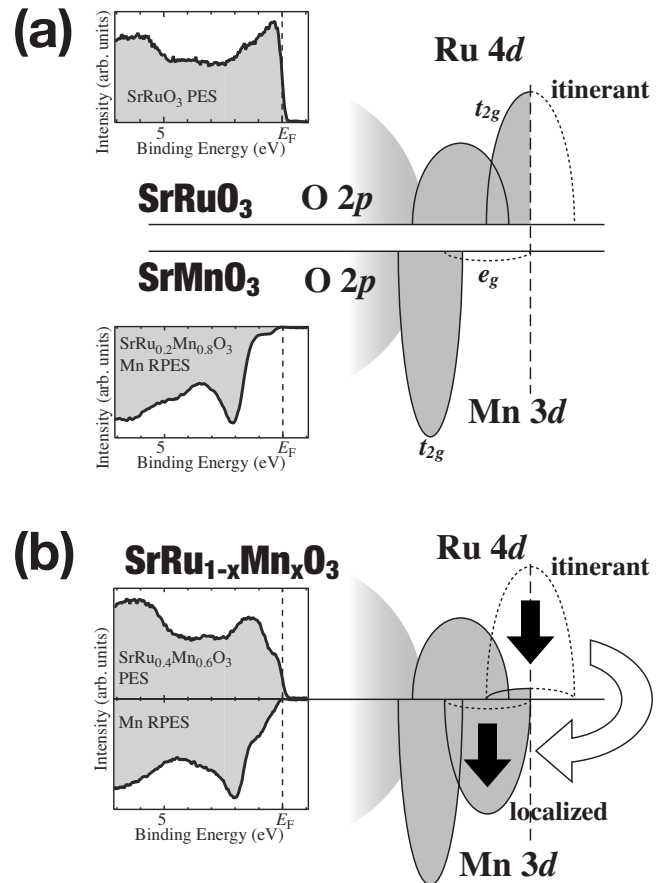


FIG. 5. Schematic diagrams of the electronic structure for (a) mother compounds SrRuO_3 and SrMnO_3 , and (b) mixed compounds $\text{SrRu}_{1-x}\text{Mn}_x\text{O}_3$.

measurements for revealing the change in the electronic structure with Mn doping of SRMO. In the soft x-ray PES spectra, the sharp peak structure near E_F , which is clearly observed in SRO, is strongly suppressed accompanied with Mn doping in SRMO. In the Mn $2p$ XAS and Mn $2p$ - $3d$ resonant PES spectra, we confirm the existence of Mn³⁺ ions with the electron doping to Mn $3d$ e_g states and Mn $3d$ partial DOS never have finite intensity at E_F in SRMO. These results suggest that the metal-insulator transition of SRMO with Mn doping is originated from the charge transfer from the itinerant Ru $4d$ t_{2g} bands to the localized Mn $3d$ e_g orbitals.

This work was partly done under Project No. 2006G010 at the Institute of Materials Structure Science in KEK.

*Present address: Department of Applied Chemistry, The University of Tokyo, 7-3-1 Hongo, Bunkyo-ku, Tokyo 113-8656, Japan; horiba@sr.t.u-tokyo.ac.jp

¹M. Imada, A. Fujimori, and Y. Tokura, *Rev. Mod. Phys.* **70**, 1039 (1998).

²Y. Tokura, *Colossal Magnetoresistive Oxides*, Advances in Con-

densed Matter Science (Gordon and Breach, Amsterdam, 2000), Vol. 2.

³K. W. Kim, J. S. Lee, T. W. Noh, S. R. Lee, and K. Char, *Phys. Rev. B* **71**, 125104 (2005).

⁴J.-H. Kim, J.-Y. Kim, B.-G. Park, and S.-J. Oh, *Phys. Rev. B* **73**, 235109 (2006).

- ⁵A. J. Williams, A. Gillies, J. P. Attfield, G. Heymann, H. Huppertz, M. J. Martínez-Lope, and J. A. Alonso, *Phys. Rev. B* **73**, 104409 (2006).
- ⁶L. Pi, A. Maignan, R. Retoux, and B. Raveau, *J. Phys.: Condens. Matter* **14**, 7391 (2002).
- ⁷G. Cao, S. Chikara, X. N. Lin, E. Elhami, V. Durairaj, and P. Schlottmann, *Phys. Rev. B* **71**, 035104 (2005).
- ⁸R. K. Sahu, Z. Hu, M. L. Rao, S. S. Manoharan, T. Schmidt, B. Richter, M. Knupfer, M. Golden, J. Fink, and C. M. Schneider, *Phys. Rev. B* **66**, 144415 (2002).
- ⁹M. Yokoyama, C. Satoh, A. Saitoh, H. Kawanaka, H. Bando, K. Ohoyama, and Y. Nishihara, *J. Phys. Soc. Jpn.* **74**, 1706 (2005).
- ¹⁰X. Y. Zhang, Y. Chen, Z. Y. Li, C. Vittoria, and V. G. Harris, *J. Phys.: Condens. Matter* **19**, 266211 (2007).
- ¹¹X.-Y. Zhang, Y. Chen, H.-X. Cao, Z.-Y. Li, and C. K. Ong, *Solid State Commun.* **145**, 259 (2008).
- ¹²S. Kolesnik, B. Dabrowski, and O. Chmaissem, *Phys. Rev. B* **78**, 214425 (2008).
- ¹³Z. H. Han, J. I. Budnick, W. A. Hines, B. Dabrowski, and T. Maxwell, *Appl. Phys. Lett.* **89**, 102501 (2006).
- ¹⁴Y. Hikita, L. F. Kourkoutis, T. Susaki, D. A. Muller, H. Takagi, and H. Y. Hwang, *Phys. Rev. B* **77**, 205330 (2008).
- ¹⁵K. Horiba, N. Kamakura, K. Yamamoto, K. Kobayashi, and S. Shin, *J. Electron Spectrosc. Relat. Phenom.* **144-147**, 1027 (2005).
- ¹⁶M. Abbate, F. M. F. de Groot, J. C. Fuggle, A. Fujimori, O. Strebel, F. Lopez, M. Domke, G. Kaindl, G. A. Sawatzky, M. Takano, Y. Takeda, H. Eisaki, and S. Uchida, *Phys. Rev. B* **46**, 4511 (1992).
- ¹⁷C. Mitra, Z. Hu, P. Raychaudhuri, S. Wirth, S. I. Csiszar, H. H. Hsieh, H.-J. Lin, C. T. Chen, and L. H. Tjeng, *Phys. Rev. B* **67**, 092404 (2003).
- ¹⁸Z. Hu, M. S. Golden, S. G. Ebbinghaus, M. Knupfer, J. Fink, F. M. F. de Groot, and G. Kaindl, *Chem. Phys.* **282**, 451 (2002).
- ¹⁹J. J. Yeh and I. Lindau, *At. Data Nucl. Data Tables* **32**, 1 (1985).
- ²⁰K. Horiba *et al.* (unpublished).
- ²¹K. Ebata, H. Wadati, M. Takizawa, A. Fujimori, A. Chikamatsu, H. Kumigashira, M. Oshima, Y. Tomioka, and Y. Tokura, *Phys. Rev. B* **74**, 064419 (2006).
- ²²M. Takizawa, D. Toyota, H. Wadati, A. Chikamatsu, H. Kumigashira, A. Fujimori, M. Oshima, Z. Fang, M. Lippmaa, M. Kawasaki, and H. Koinuma, *Phys. Rev. B* **72**, 060404(R) (2005).
- ²³K. Horiba, A. Chikamatsu, H. Kumigashira, M. Oshima, N. Nagakawa, M. Lippmaa, K. Ono, M. Kawasaki, and H. Koinuma, *Phys. Rev. B* **71**, 155420 (2005).